Progress In Electromagnetics Research Letters, Vol. 99, 75–81, 2021

Cost-Effective Compact Dual-Band Patch Antenna Based on Ball Grid Array Packaging for 5G mmWave

Xiubo Liu[1], Wei Zhang[1], Dongning Hao[1], and Yanyan Liu[2, *]

Abstract—In this letter, a compact dual-band patch antenna based on ball grid array (BGA) packaging for 5G mmWave is proposed. The patch antenna adopts a U-slot and a shorting pin to achieve dual-band operation of 28 GHz and 37 GHz. A single-layer FR4 substrate provides cost-effective features for the massive application. The BGA packaging not only reduces the size but also enables the antenna to be surface-mounted with other components in the same package, which improves the integration. The antenna has been fabricated and measured, and an acceptable agreement was obtained between the simulation and measurement results.

1. INTRODUCTION

The fifth generation (5G) millimeter-wave frequency band includes massive bandwidth and provides high-rate coverage to overcome the challenge of mobile data growth. Due to the strong path loss and the high absorption of atmospheric and rain in the millimeter-wave, the density of the 5G millimeter-wave wireless system is higher than that of the previous four generations [1, 2]. Therefore, low-cost antennas are more attractive for 5G millimeter-wave applications. On the other hand, it is a great challenge to face the strong path loss, atmospheric and rain absorption in the millimeter-wave spectrum. However, for small distance cellular propagation (less than 1 km), atmospheric absorption and rain attenuation show minimal effect on 28 GHz to 38 GHz. When the rain rate is 1 inch/hr, the attenuation is about 7 dB/km [2, 3]. Therefore, the 28 GHz and 38 GHz frequency bands are good candidate frequency bands for 5G millimeter waves. The dual-frequency antenna can work in two different frequency bands, with a small size and easy integration. Several studies on dual-band antennas at 28 GHz and 38 GHz have been carried out, such as dual-band arrays based on coupled quarter-mode substrate-integrated waveguide [4], patch antenna with pairs of shorting pins and H-shaped slot in [5], and planar omnidirectional antenna [6].

Microstrip patch antennas have become a commonly used antenna in wireless systems due to their advantages of low cost, simple structure, and easy fabrication [7–12]. To reduce the antenna size, the shorting pin is added to obtain a compact size [8, 9]. To overcome the shortcomings of narrow bandwidth, a U-slot is used to improve the bandwidth of the patch antenna [7, 8]. However, one of the main challenges of the above-mentioned antennas is the interconnection between the antenna and the RF front-end chipset. Interconnection requires a coaxial connector for connection, but coaxial connectors have high insertion loss and are difficult to integrate. Antenna-in-Package (AiP) technology based on BGA packaging has the advantage of easy integration and low-loss interconnection [13–15]. It can replace high insertion loss connectors for better performance.

Inspired by the above results, this letter proposes a dual-band patch antenna based on BGA packaging for the 5G mmWave applications. Based on our previous research [16], the proposed antenna achieves compact size by using BGA packaging. The antenna uses a single FR4 substrate, which reduces

Received 12 June 2021, Accepted 26 July 2021, Scheduled 2 August 2021

* Corresponding author: Yanyan Liu (lyytianjin@nankai.edu.cn).

[1] School of Microelectronics, Tianjin University, Tianjin 300072, China. [2] Tianjin Key Laboratory of Photo-electronic Thin Film Devices and Technology, Nankai University, Tianjin 300071, China.

the cost. Moreover, the low-frequency resonant is achieved by the shorting pin based on plated through-hole (PTH), and the high-frequency resonant is realized by the U-slot coupling. The prototype has been designed, fabricated, and verified. All simulation results are given by ANSYS electromagnetics.

2. ANTENNA DESIGN

2.1. Antenna Geometry

Figure 1 depicts the geometry of the proposed dual-band antenna. Only one layer of FR4 is used with a permittivity of 4.4, dielectric loss tangent of 0.02, and thickness of 1.5 mm to obtain the low cost. Two metal layers are etched on either side of the dielectric layer to serve as the top and bottom layers. As shown in Figure 1(b), a U-slot is etched on the top metal layer. Besides, a feedline is etched on the bottom metal layer to form the grounded coplanar waveguide (GCPW) transmission line. There are two plated through holes inside the substrate. One transmits the radio frequency (RF) signals from the bottom feedline to the top patch, and the other connects the patch layer to the bottom ground layer. Then the solder resists layer is coated on the bottom metal layer, and the solder balls are mounted on the bottom layer of the antenna to complete the BGA packaging. The detailed dimensions of the proposed antenna element are listed in Table 1. The final size is 5 mm × 3 mm × 1.7 mm.

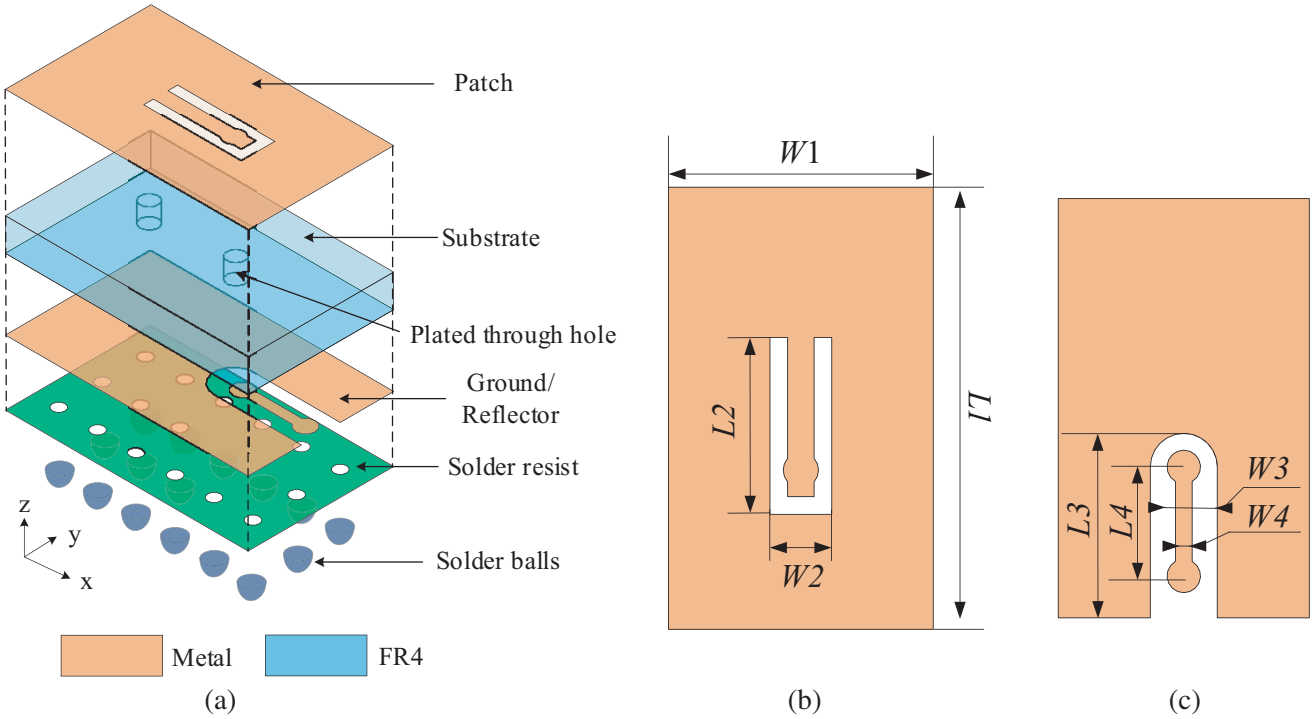

Figure 1. Geometry of the proposed antenna element. (a) Explored view. (b) Top view. (c) Bottom view.

Table 1. Dimensions of the proposed antenna element (Units: mm).

Parameters	Values	Parameters	Values
$L1$	5	$W1$	3
$L2$	2	$W2$	0.7
$L3$	2.2	$W3$	0.8
$L4$	1.3	$W4$	0.2

2.2. Simulated Results

The simulated reflection coefficient, peak gain, and efficiency are shown in Figure 2, respectively. The simulated impedance bandwidth of $|S_{11}| < -10$ dB ranges from 27.9 to 28.9 GHz and 36.3 to 37.9 GHz. In the low-frequency band, the simulated gain is above 3.18 dBi, and the peak gain at 27.5 GHz is 3.71 dBi. The simulated efficiency is 71.6%–80.7%. In the high-frequency band, the simulated gain is 4.56–4.96 dBi, and the efficiency is 74.6%–76.4%. Figure 3 shows the simulated E-plane (XOZ) and H-plane (YOZ) normalized radiation patterns at 28.5 GHz, and 37 GHz, respectively. It can be observed that the cross-polarization levels of the main beam at 28.5 GHz and 37 GHz are lower than 35 dB and 33.8 dB, respectively.

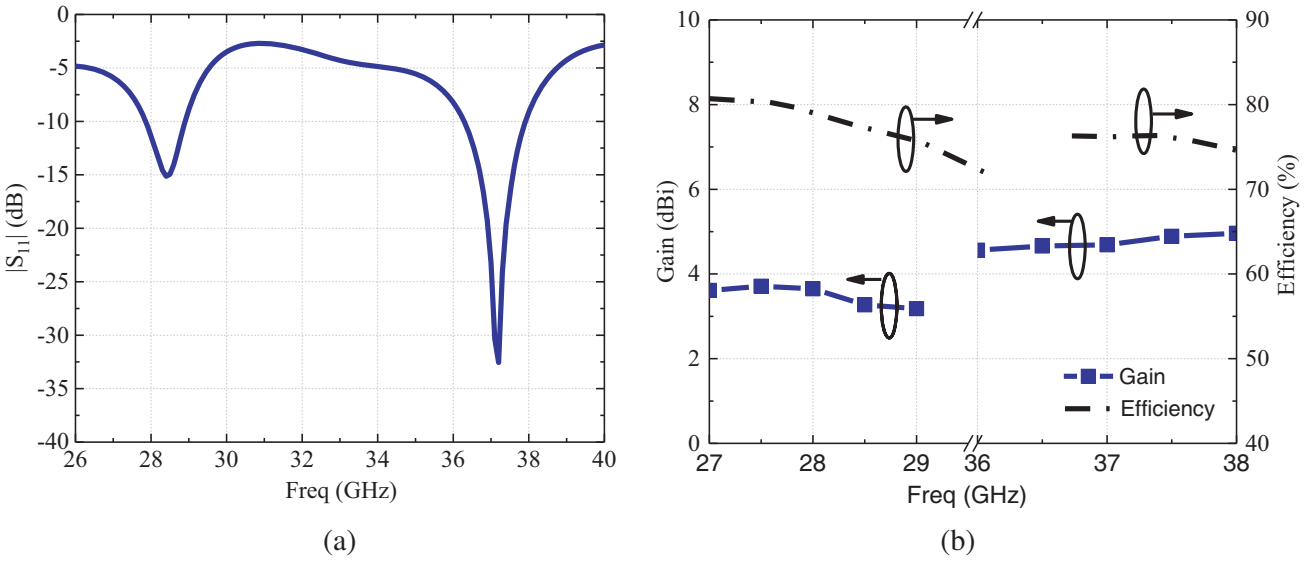

Figure 2. (a) Simulated reflection coefficient of the proposed antenna. (b) Simulated gain and efficiency of the proposed antenna.

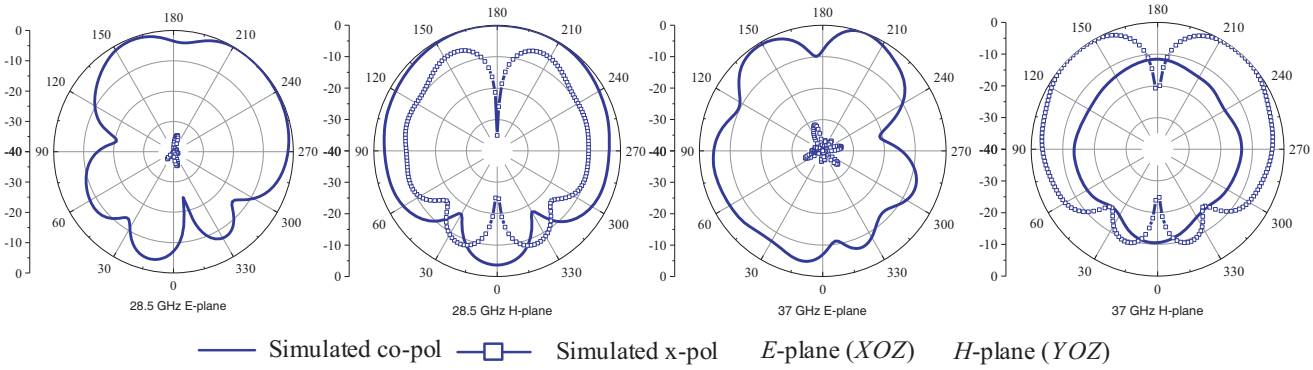

Figure 3. Simulated E-plane and H-plane normalized radiation patterns at 28.5 GHz, and 37 GHz.

2.3. Parametric Analysis

Figure 4 shows the surface current distribution of the proposed antenna element at a low frequency of 28.5 GHz and a high frequency of 37 GHz, respectively. At 28 GHz, the surface current is mainly concentrated around the shorting pin. In addition, part of the current is distributed in the opposite direction along the edge of the patch. At 36 GHz, the surface current is mainly distributed around the

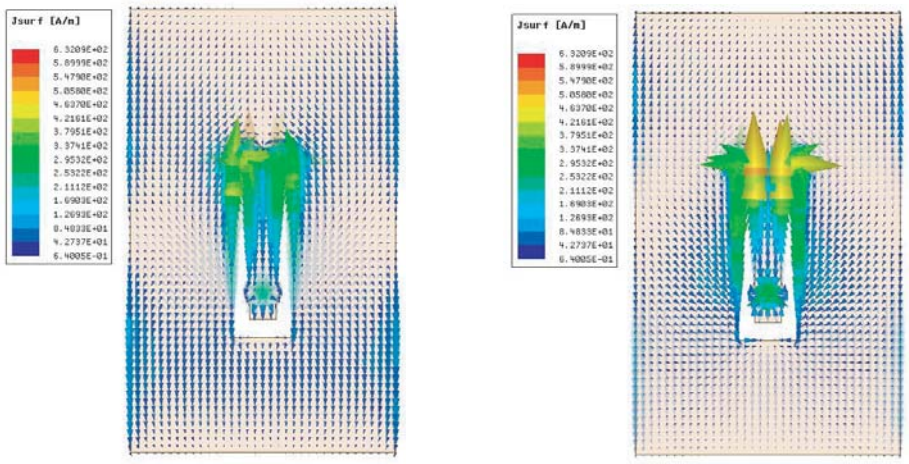

(a) (b)

Figure 4. Surface current distribution of the proposed antenna element. (a) 28.5 GHz. (b) 37 GHz.

U-slot, and the current distribution along the edge is relatively small. It can be seen that the shorting pin with inductive load has a greater effect on the low-frequency band, while the U-slot has a greater effect on the high-frequency band.

Within the millimeter-wave frequency band, the manufacturing tolerance has a great influence on the antenna performance. As shown in Figure 5, $W4$ and $L1$ were analyzed. The scan value of $W4$ is in the range of 0.1–0.4 mm, and $L1$ is in the range of 5–5.4 mm. When one of the parameters is simulated, the others remain at their optimal values. It can be seen that the low-frequency reflection coefficient will be affected when $W4$ decreases, while the high-frequency reflection coefficient will be affected when $W4$ increases. In addition, as $L1$ increases, the band will move to a lower frequency. To maintain balance, $W4$ is set to 0.2 mm, and L1 is set to 5 mm.

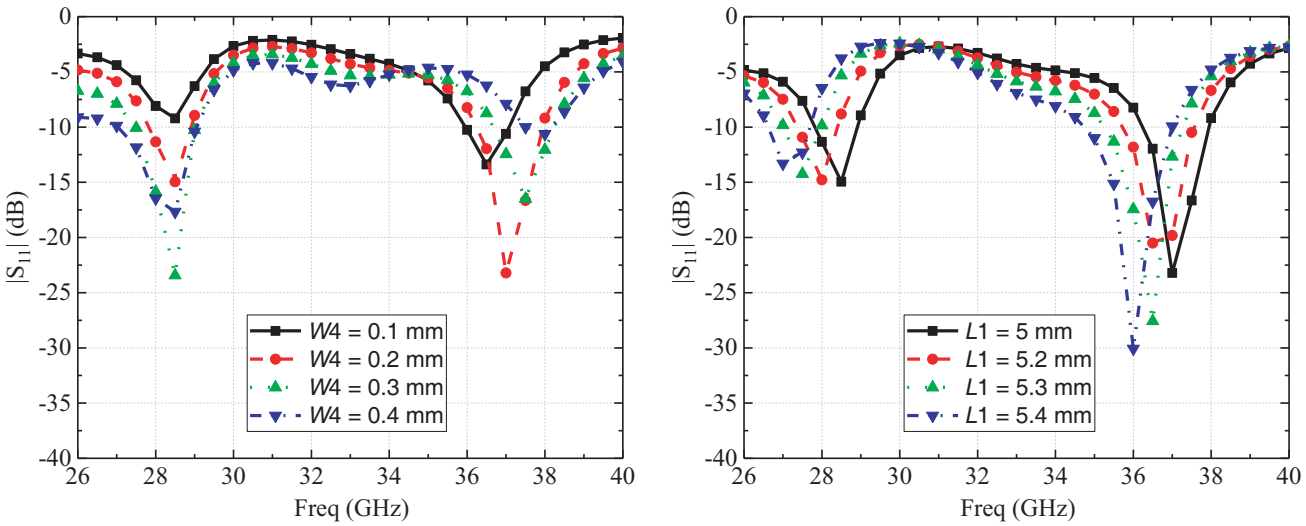

(a) (b)

Figure 5. Simulated $|S_{11}|$ of the antenna element with different parameters. (a) $W4$. (b) $L1$.

3. MEASUREMENT RESULTS AND DISCUSSION

As shown in Figure 6, a prototype was made to verify the performance. The prototype is fed by the evaluation board made on Rogers 4350B with a thickness of 0.254 mm. A 2.92 mm connector is mounted on the edge of the evaluation board and connects to Rohde & Schwarz's vector network analyzer (ZVA40) for the reflection coefficient measurement. Radiation patterns are measured in an anechoic chamber.

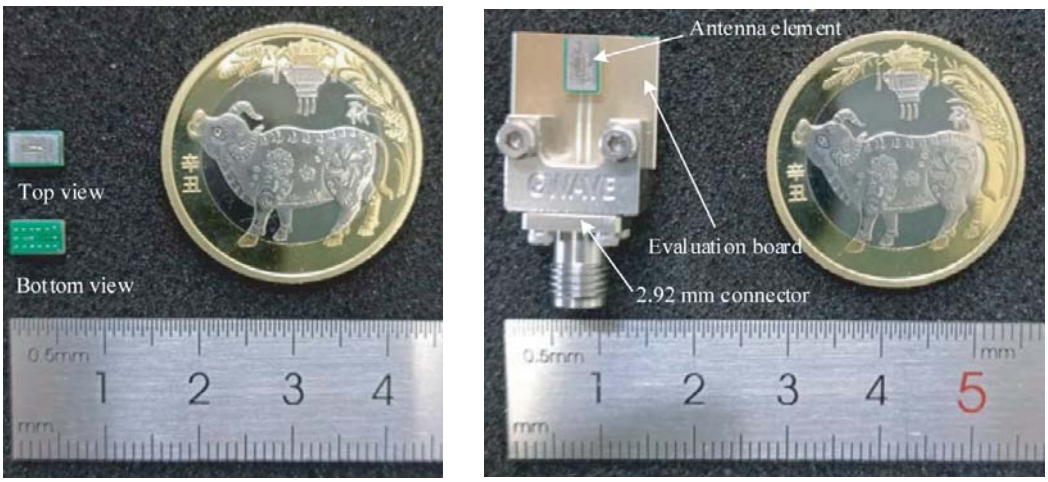

(a) (b)

Figure 6. Photograph of the dual band antenna prototype. (a) Antenna element. (b) Assembly prototype.

The measured reflection coefficients and gain are shown in Figure 7(a) and Figure 7(b), respectively. The reflection coefficient of the $|S_{11}| < -10$ dB covers 26.8–27.5 GHz, and 35.1–36.4 GHz. The measured prototype has a peak gain of 5.49 dBi at 27 GHz and 4.26 dBi at 36 GHz. Figure 8 shows the measured E-plane (XOZ) and H-plane (YOZ) normalized radiation patterns at 27 GHz and 36 GHz, respectively. Compared with the simulation results, it can be seen that the resonance point has shifted to low frequency.

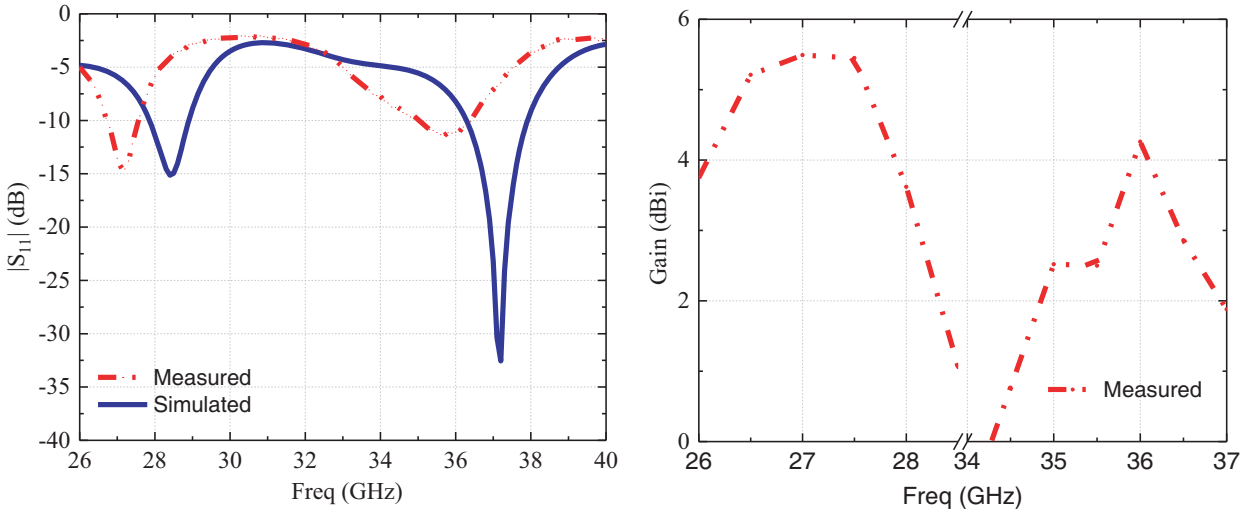

(a) (b)

Figure 7. (a) Measured reflection coefficient. (b) Measured peak gain.

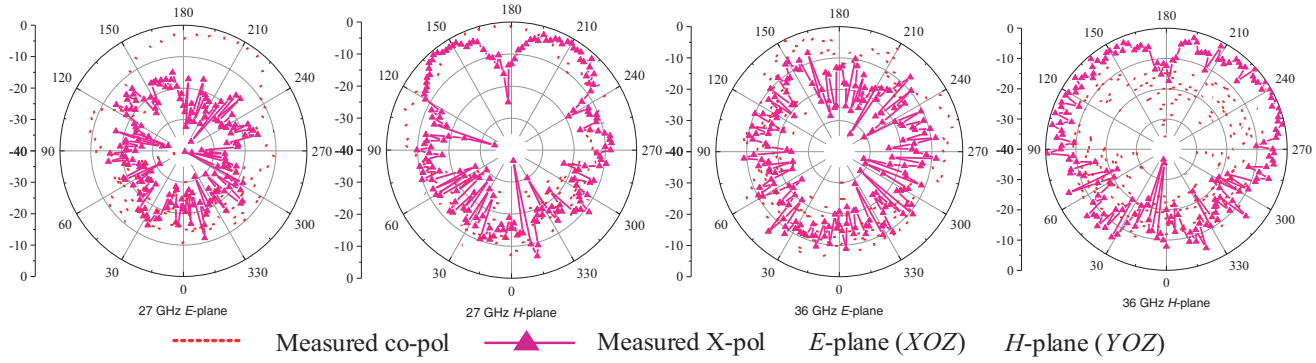

Figure 8. Measured E-plane and H-plane normalized radiation patterns at 27 GHz, and 36 GHz.

In addition, as shown in Figure 8, the E-plane cross-polarization levels of the main beam measured at 28.5 GHz and 37 GHz are lower than 23.6 dB and 10.9 dB, respectively. Compared to the simulation result, the measurement result has deteriorated. The cross-polarization level of the H-plane is greater than the co-polarization, especially at 36 GHz. Based on the above parameter analysis, this difference is mainly caused by manufacturing tolerances. Due to the difficulty of PCB small size processing, $L1$ is larger than the design value, resulting in frequency deviation. On the other hand, the dielectric loss of the substrate is small compared with the design value, which leads to a little large antenna gain.

Table 2 shows the comparison between the proposed antenna and the reporting antenna. It can be seen that the proposed antenna is fabricated on a low-cost FR4 substrate, which has the advantage of cost-effectiveness. Secondly, the interconnection between the antenna and the RF chipset in [4–6] must use a bulky and lossy connector, which is difficult to integrate. The proposed antenna is based on the BGA packaging and has a compact size. Most importantly, the BGA package allows the proposed antenna to be easily integrated with the RF chipset without the need for any bulky connectors.

Table 2. Comparisons between the proposed and reported antennas.

Ref.	No. of elements	Spectrum (GHz)		FBW (%)		Element size (mm^3)	Material
		Low band	High band	Low band	High band		
[4]	1×4	27.5–29.5	37–38.6	7	4.2	$4.48 \times 3.79 \times 0.526$	Duroid 5880
[5]	1×1	27.7–28.7	36.8–40.2	3.5	8.8	25×15	Taconic TLY-5
[6]	1×1	26.65–29.2	36.95–39.05	9.13	5.52	$14 \times 12 \times 0.38$	RT/Duroid 5880
This work	1×1	26.8–27.5	35.1–36.4	2.6	3.6	$5 \times 3 \times 1.7$	FR4

4. CONCLUSIONS

A cost-effective dual-band antenna for 28 and 37 GHz based on BGA packaging has been proposed. The antenna prototype has been simulated, manufactured, and verified. To achieve a cost-effective feature, FR4 is used as the antenna substrate. In addition, the BGA packaging makes the proposed antenna compact in size and easy to integrate. For measurement purposes, the evaluation board is made on RO4350B to verify the antenna performance. The low-frequency band is achieved by the shorting pin with inductive loads. The high-frequency band is realized by U-slot coupling. The measurement results confirm that -10 dB bandwidth of the low-frequency band is 3.8% and 9.0% at the high-frequency band. An acceptable agreement was obtained between simulation and measurement results. The cost-effective characteristics and compact size make the proposed antenna one of the candidates for 5G millimeter-wave applications.

ACKNOWLEDGMENT

The authors would like to thank Prof. Hongxing Zheng of the School of Electronics and Information Engineering, Hebei University of Technology, for helping with the antenna measurements.

REFERENCES

1. Andrews, J. G., et al., "What will 5G be?" *IEEE J. Sel. Areas Commun.*, Vol. 32, No. 6, 1065–1082, Jun. 2014.
2. Rappaport, T. S., et al., "Millimeter wave mobile communications for 5G cellular: It will work!," *IEEE Access*, Vol. 1, 335–349, 2013.
3. Zhao, Q. and J. Li, "Rain attenuation in millimeter wave ranges," *2006 7th International Symposium on Antennas, Propagation EM Theory*, 1–4, Oct. 2006.
4. Deckmyn, T., M. Cauwe, D. V. Ginste, H. Rogier, and S. Agneessens, "Dual-band $(28, 38)$ GHz coupled quarter-mode substrate-integrated waveguide antenna array for next-generation wireless systems," *IEEE Trans. Antennas Propag.*, Vol. 67, No. 4, 2405–2412, Apr. 2019.
5. Liu, P., X. Zhu, Y. Zhang, X. Wang, C. Yang, and Z. H. Jiang, "Patch antenna loaded with paired shorting pins and H-shaped slot for 28/38 GHz dual-band MIMO applications," *IEEE Access*, Vol. 8, 23705–23712, 2020.
6. Hasan, M. N., S. Bashir, and S. Chu, "Dual band omnidirectional millimeter wave antenna for 5G communications," *Journal of Electromagnetic Waves and Applications*, Vol. 33, No. 12, 1581–1590, 2019.
7. Carver, K. and J. Mink, "Microstrip antenna technology," *IEEE Trans. Antennas Propag.*, Vol. 29, No. 1, 2–24, Jan. 1981.
8. Telsang, T. M. and A. B. Kakade, "Ultrawideband slotted semicircular patch antenna," *Microw. Opt. Technol. Lett.*, Vol. 56, No. 2, 362–369, 2014.
9. Waterhouse, R. B., S. D. Targonski, and D. M. Kokotoff, "Design and performance of small printed antennas," *IEEE Trans. Antennas Propag.*, Vol. 46, No. 11, 1629–1633, Nov. 1998.
10. Kaur, K., A. Kumar, and N. Sharma, "Split ring slot loaded compact CPW-fed printed monopole antennas for ultra-wideband applications with band notch characteristics," *Progress In Electromagnetics Research C*, Vol. 110, 39–54, 2021.
11. Liu, S., S.-S. Qi, W. Wu, and D.-G. Fang, "Single-layer single-patch four-band asymmetrical U-slot patch antenna," *IEEE Trans. Antennas Propag.*, Vol. 62, No. 9, 4895–4899, Sep. 2014.
12. Mok, W. C., S. H. Wong, K. M. Luk, and K. F. Lee, "Single-layer single-patch dual-band and triple-band patch antennas," *IEEE Trans. Antennas Propag.*, Vol. 61, No. 8, 4341–4344, Aug. 2013.
13. Zhang, Y. P., "Integration of microstrip patch antenna on ceramic ball grid array package," *Electron. Lett.*, Vol. 38, No. 5, 207–208, Feb. 2002.
14. Sun, M., Y. P. Zhang, D. Liu, K. M. Chua, and L. L. Wai, "A ball grid array package with a microstrip grid array antenna for a single-chip 60-GHz receiver," *IEEE Trans. Antennas Propag.*, Vol. 59, No. 6, 2134–2140, Jun. 2011.
15. Zhang, Y. P., "Integrated circuit ceramic ball grid array package antenna," *IEEE Trans. Antennas Propag.*, Vol. 52, No. 10, 2538–2544, Oct. 2004.
16. Liu, X., W. Zhang, D. Hao, and Y. Liu, "A compact broadband folded dipole antenna element with ball grid array packaging for new 5G application," *Progress In Electromagnetics Research Letters*, Vol. 96, 113–119, 2021.